SEMARAK ILMU PUBLISHING

Journal of Advanced Research in Fluid Mechanics and Thermal Sciences

Journal homepage:
https://semarakilmu.com.my/journals/index.php/fluid_mechanics_thermal_sciences/index
ISSN: 2289-7879

Blood Flow Acoustics in Carotid Artery

Salman Aslam Ramdan[1], Mohammad Rasidi Rasani[1,*], Thinesh Subramaniam[1], Ahmad Sobri Muda[2], Ahmad Fazli Abdul Aziz[3], Tuan Mohammad Yusoff Shah Tuan Ya[4], Hazim Moria[5], Mohd Faizal Mat Tahir[1], Mohd Zaki Nuawi[1]

[1] Department of Mechanical and Manufacturing Engineering, Faculty of Engineering and Built Environment, Universiti Kebangsaan Malaysia, 43600 Bangi, Selangor, Malaysia
[2] Department of Radiology, Faculty of Medicine and Health Sciences, Universiti Putra Malaysia, 43400 Serdang, Selangor, Malaysia
[3] Department of Medicine, Faculty of Medicine and Health Sciences, Universiti Putra Malaysia, 43400 Serdang, Selangor, Malaysia
[4] Department of Mechanical Engineering, Faculty of Engineering, Universiti Teknologi Petronas, 32610 Seri Iskandar, Perak, Malaysia
[5] Department of Mechanical Engineering Technology, Yanbu Industrial College, Yanbu Al-Sinaiyah City 41912, Saudi Arabia

ARTICLE INFO

Article history:
Received 7 November 2021
Received in revised form 25 February 2022
Accepted 9 March 2022
Available online 2 April 2022

Keywords:
Computational Fluid Dynamics (CFD); Stenosis; Carotid Artery; Bifurcation; Blood flow

ABSTRACT

This paper aims to identify and study the blood flow and acoustics characteristics of different degrees of stenosis in the carotid artery. Blood flow will produce acoustics, but the presence of different levels of stenosis are expected to produce different acoustic characteristics. The blood flow and acoustic characteristics are simulated by using computational fluid dynamics software (CFD). Several three-dimensional models of carotid arteries that have different degrees of stenosis are used together with a normal/healthy carotid artery - i.e., 30% and 70% degrees of blockage. The geometry of 30% and 70% stenosed model are computationally generated from a normal carotid artery geometry. In addition, the blood viscosity level was also increased in this study to a value of 0.005 $kgms^{-1}$ (from the normal viscosity of 0.004 $kgms^{-1}$) to compare the effect of hyperglycaemia (i.e., diabetes mellitus) that may bring additional complications to blood flow. Pulsatile simulations are used for all cases in order to mimic the exact blood flow condition in which the inlet velocity and outlet pressure change with time. The present study shows that as the degree of stenosis increases at the common carotid artery (CCA), the velocity at the internal carotid artery (ICA) and external carotid artery (ECA) outlet increases. The maximum velocity changes for ICA at the systolic peak from normal to 70% degree of stenosis for carotid artery shows an increase by 8%, while an opposite trend is observed for the maximum velocity changes of ECA at the systolic peak, where a reduction by 3% occurs from normal to 70% degree of stenosis for carotid artery. In terms of viscosity, as the viscosity of the blood increases, the velocity of the blood flow decreases in all geometry carotid arteries and may potentially provide further complications on clinical problems. The acoustic simulation showed that the acoustic power increases by 5% and 20% for carotid artery geometry that has 30% and 70% degree of stenosis, respectively. The present study indicates potential for further developing non-invasive acoustic means to diagnose and measure stenosis in carotid arteries.

* *Corresponding author.*
E-mail address: rasidi@ukm.edu.my

https://doi.org/10.37934/arfmts.94.1.2844

1. Introduction

Blood flow is associated with many cardiovascular problems and strokes [1]. The narrowing of the blood vessels called stenosis is caused by the formation of plaque inside the vascular wall, which can lead to the reduction of blood flow in the arteries and will affect the amount of blood supplied to the brain that will lead to strokes [2]. This atherosclerosis can occur in all blood vessels in the body. Blood flow produces a sound characterized by a sound or brute [3]. Researchers agreed that most of the source of the discharge came from interference in blood flow resulting from the existence of obstructions in the blood vessels [4]. In addition, the degree of stenosis obstructions in the blood vessels will produce different acoustic features [5]. Therefore, hemodynamics related to this drainage needs to be studied more deeply considering the spread and release of waves in the blood vessels. Carotid artery bifurcation, which divides blood flow into two branches - Internal Carotid Artery (ICA) and External Carotid Artery (ECA), is shown in Figure 1.

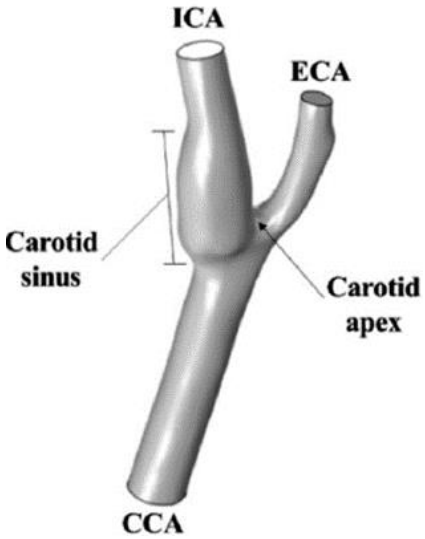

Fig. 1. Geometry of carotid artery bifurcation showing common carotid artery (CCA), internal carotid artery (ICA) and external carotid artery (ECA) [6]

Computational Fluid Dynamics (CFD) numerical simulation is a valid approach for solving and analysing blood flow problems because it can replicate results that are consistent with those obtained in in-vivo studies. For such simulations to be successful, accurate anatomic models must be used, realistic boundary conditions must be imposed, an appropriate viscosity model must be used, and the wall elasticity must be taken into consideration.

In previous studies, computational fluid dynamics (CFD) simulation in three-dimensional models that are produced from anatomic medical scanning images has been applied to analyse the blood flow in a number of arteries (see examples in the studies by Chen *et al.,* [7], Zakaria *et al.,* [8], and Khader *et al.,* [9]). In order to fully understand the complicated nature of the stenosis carotid bifurcation and its impact on blood flow patterns, investigations with patient-specific geometries are essential [10]. Interestingly, Lopes *et al.,* [11] conducted a systematic literature evaluation of carotid artery numerical simulation with patient-specific geometries that can understand the studies on the geometry of carotid arteries.

Several studies prove there are significant differences in comparison between Newtonian and non-Newtonian models, namely differences in local hemodynamics in critical areas such as carotid sinuses [12,13]. The findings showed the suitability of non-Newtonian model as blood flow model for carotid artery simulation studies [11]. Some of the models previously considered include Casson fluid model (the theory of which may be found in for example in the studies by Sarifuddin [14], and Yusof *et al.,* [15]), Herschel-Bulkley, power law and Carreau-Yasuda rheological models. However, Newtonian models may still be reasonable for large arteries with relatively high shear rates [9]. Based on previous studies, the assumption that blood flow is laminar in healthy models of carotid artery patients is appropriate at the beginning of the study [16]. However, new studies have shown that the geometry of the carotid artery with a higher degree of stenosis should be applied with a flow from transition to turbulence [17]. Furthermore, in terms of boundary conditions, the majority of studies that use patient-specific parameters will produce more realistic results than studies using presumed parameters.

One of the major risk factors leading to stroke is the narrowing (stenosis) or obstruction of carotid arteries. This narrowing may either (i) directly reduce flow of blood to brain or (ii) if the narrowing is caused by plaque formation, these plaques may be dislodged by the blood flow and travel downstream blocking smaller blood vessels that supply blood to the brain. Current diagnosis of carotid artery stenosis includes doppler ultrasound, CT angiography or magnetic resonance angiography, which are relatively costly and involve expensive equipment, which may not be available at all hospitals/clinics. As varying degree of stenosis are expected to generate different acoustic features, developing a relatively inexpensive and portable acoustic-based diagnosis tool may allow more practical and wider screening of this particular risk factor to stroke.

In addition, people with diabetes are at higher risk to have stroke. Since diabetes leads to hyperglycemia (elevated blood glucose levels) that affects the viscosity of blood, it would also be necessary to investigate effects of viscosity on the generated flow acoustics.

Therefore, this study is performed based on the influence from previous studies and a number of aspects that have not been discussed, which include the different degrees of pre-bifurcation stenosis and effect of blood viscosity, towards blood flow characteristics and their corresponding flow-generated acoustics. The objectives of this study are summarized as follows:

i. To study the effect of different degrees of carotid artery stenosis on blood flow characteristics using computational fluid dynamics (CFD) software.
ii. To identify the effect of different degrees of carotid artery stenosis on acoustics produced using computational fluid dynamics (CFD) software.
iii. To identify the effect of high blood viscosity on blood flow and acoustic characteristics produced.

2. Methodology

A computational approach is adopted in the present study. Figure 2 shows the flowchart and approach of the present investigation. Furthermore, this research uses simulation methods that include the boundary conditions that are relevant to this analysis. The boundary condition used is based on data from relevant previous studies using Ansys Fluent software in order to compare the result as well as to successfully achieve the objectives. Data collection and interpretation processes are performed in accordance with the previous studies, based on the results of the simulation.

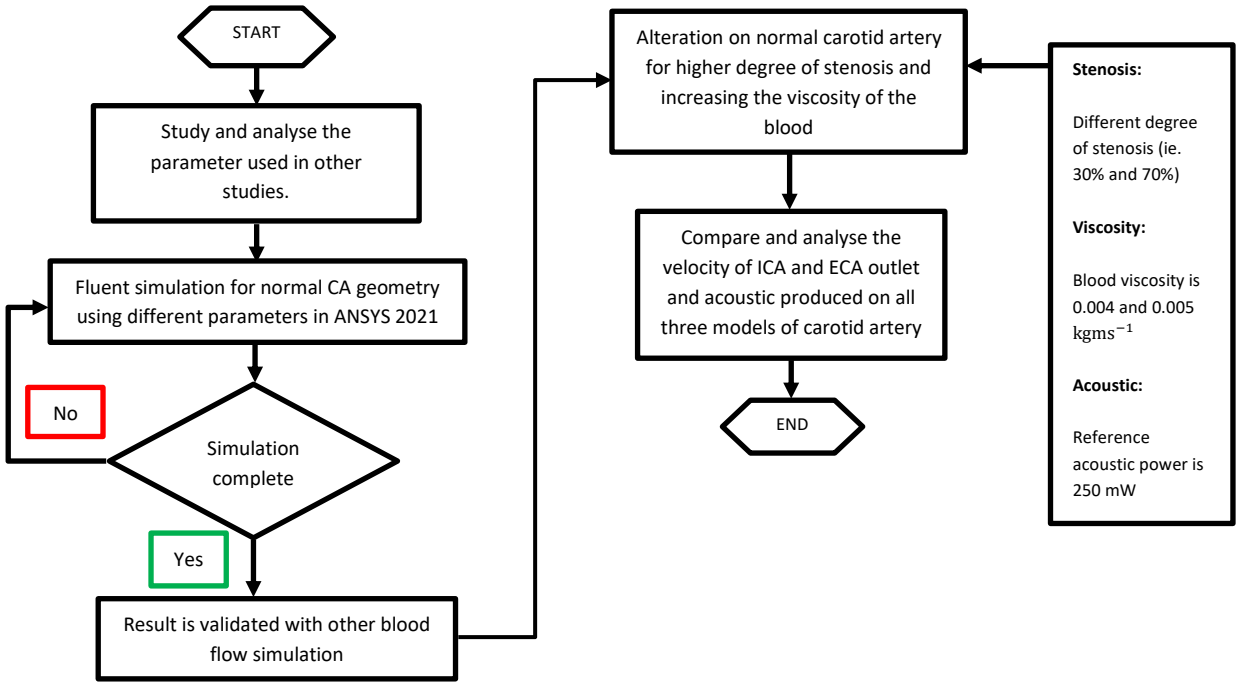

Fig. 2. Flowchart of study

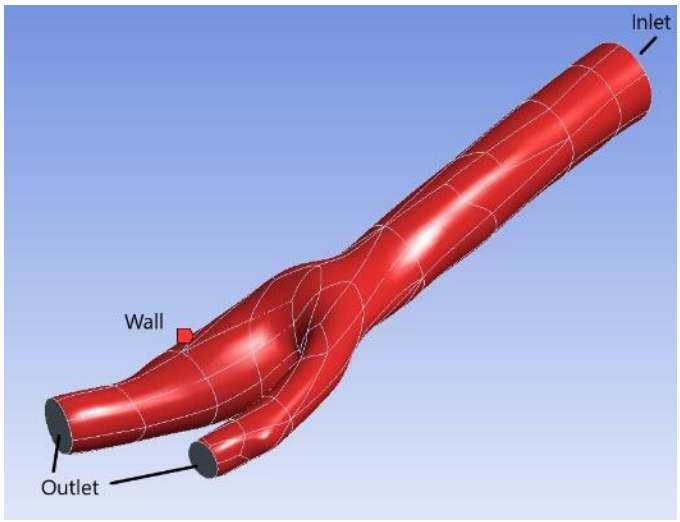

Fig. 3. Isometric view of anatomically-accurate carotid artery model used in the present study

The CFD numerical simulations were performed using ANSYS Fluent 2021 software. This study started by employing a three-dimensional model of a non-stenotic carotid artery model from previous study shown in Figure 3, that was created from a patient-specific Computed Tomography (CT) scanning. As shown in Table 1, the carotid artery wall is considered to be rigid with the no-slip condition [4]. Furthermore, the density, as well as viscosity of blood, are 1060 kgm^{-3} and 0.004 $kgms^{-1}$ [4,6], respectively. The length and width of the model are 0.055 m and 0.0017 m, as shown in Figure 4, respectively. After validating the non-stenotic/healthy blood flow simulation, a higher degree of stenosis was introduced to study the effect of different degrees of stenosis and blood viscosity on blood flow and acoustic behaviour. The results that were compared and validated on the blood flow is the velocity at the ICA and ECA outlet. The velocity magnitude of the carotid artery is measured based on the cross-section of the ICA and ECA outlet as shown in Figure 4.

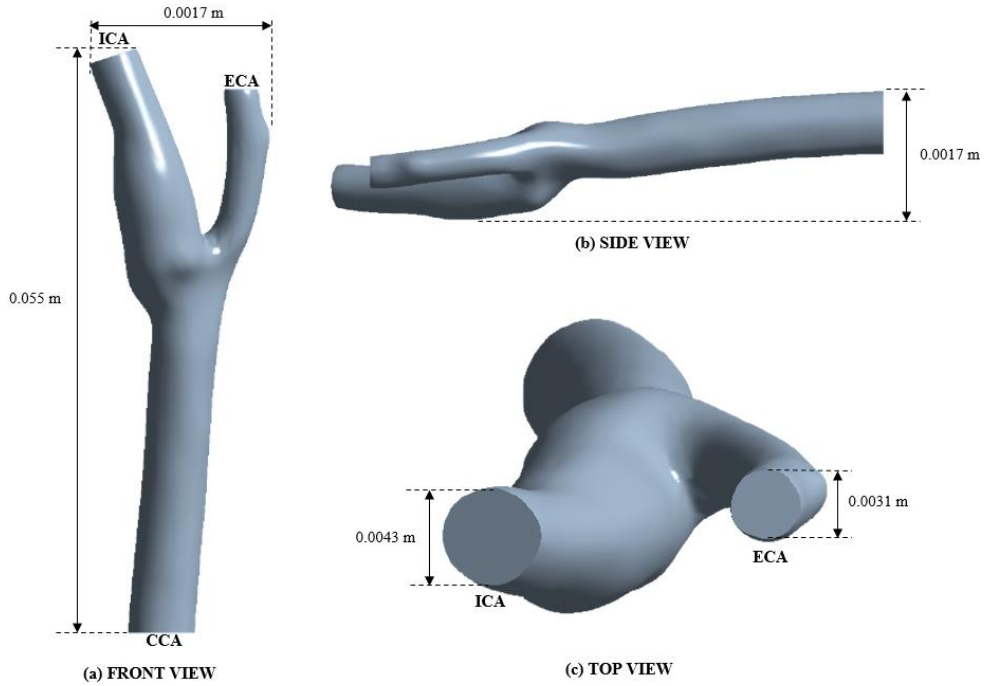

Fig. 4. Different view for the carotid artery (a) Front view (b) Side view (c) Top view

Table 1
Parameters and boundary conditions used in the present simulation

Conditions	Settings
Viscosity model	Non-newtonian
Turbulence Model	SST *k-ω* with Low Reynold's correction
Material	Blood
Viscosity of blood, $\boldsymbol{\mu}$ ($\mathbf{kgms^{-1}}$)	1. 0.004 2. 0.005
Density of blood, $\boldsymbol{\rho}$ ($\mathbf{kgm^{-3}}$)	1060
Inlet Velocity ($\mathbf{ms^{-1}}$)	Pulsatile inlet velocity
Outlet Pressure (Pa)	Pulsatile outlet pressure
Wall	Rigid with no-slip condition

The inlet velocity value is quantified by dividing the volume flowrate from Lopes *et al.,* [6] (as shown in Figure 5) by the inlet area of the carotid artery model. Other than the normal/healthy geometry of the carotid artery (CA), this study considered two different degrees of stenosis, which are 30% and 70% narrowing, in order to evaluate the effect of the different degrees of stenosis from the normal geometry, after validating the blood flow simulation. The 30% and 70% degrees of stenosis carotid artery were computationally generated based on the alteration of the normal carotid artery geometry by using ANSYS Design Modeller. The stenosis is located at the Common Carotid Artery (CCA) which is before the bifurcation (ie. pre-bifurcation). The stenosis appears on both sides of the CCA, and it is semi-circular in shape. When it comes to pre-bifurcation stenosis, the terms 30% and 70% for the degree of stenosis (DOS) are determined by the ratio of the radius of the stenosis that is limiting blood flow (A), to the cross-section radius of the healthy model (A_O), as shown in Eq. (1).

$$DOS = \frac{A}{A_0} \quad (1)$$

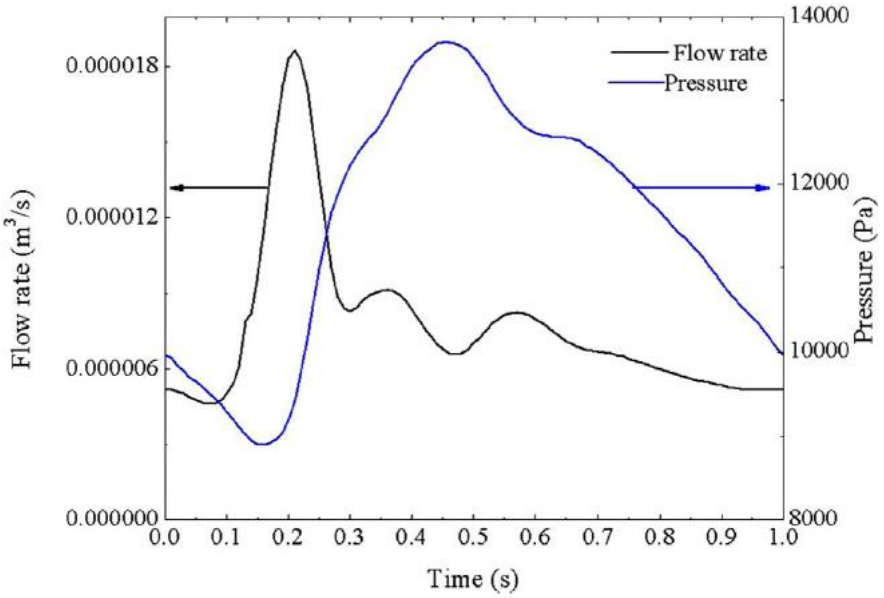

Fig. 5. Boundary conditions of the carotid artery [6]

The simulation used a pressure-based type solver. For the solution methods, SIMPLE scheme was used for the pressure-velocity coupling. In terms of spatial discretization, least-squares cell based was used for gradient, and second-order upwind is set for pressure, momentum, turbulent kinetic energy as well as specific dissipation rate. The transient formulation used was a second-order implicit scheme in order to improve the result accuracy. Moreover, this study used a transient simulation as the blood flow considered was pulsatile, in which the inlet velocity is varying with time.

A user-defined function was used in order to mimic the blood inlet velocity as well as outlet pressure at both ICA and ECA outlets. The inlet velocity, as well as outlet pressure, was adopted from Lopes *et al.,* [6]. For the model that has a degree of stenosis of 30% and 70%, the same boundary conditions were used. The size of the time-step used is 0.001 s, which complies with other studies where maximum velocity can occur at 0.20 s [6]. The simulation was run for 3 s total time, in order to simulate 3 pulses as shown in Figure 14.

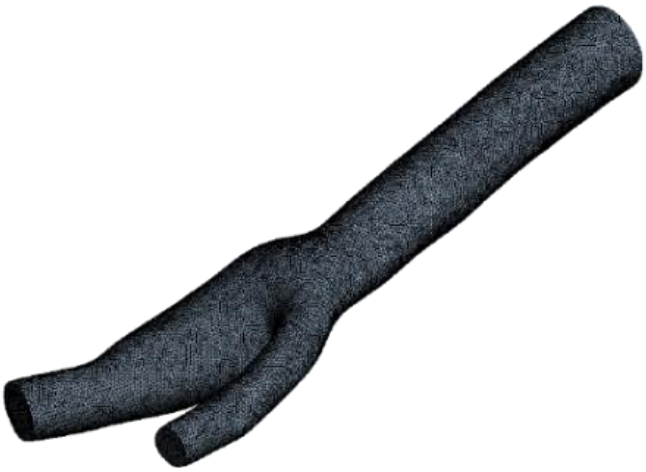

Fig. 6. Meshing on the carotid artery.

The carotid artery geometry was discretized using three-dimensional tetrahedral elements (as highlighted in Figure 6). In order to accurately resolve the boundary layer flow, 10 meshing layers that have a maximum thickness of 0.5 mm were used near the wall as highlighted in Figure 7 and Figure 8. In order to ensure that the results are not influenced by the mesh, a mesh-independence study was carried out as shown in Figure 9. The figure shows a summary of the mesh-independence study where the maximum velocity of the systolic peak at the ICA outlet is measured based on four different mesh sizing, which were from 0.26 m to 0.23 m.

Fig. 7. Mesh cross-section for carotid artery

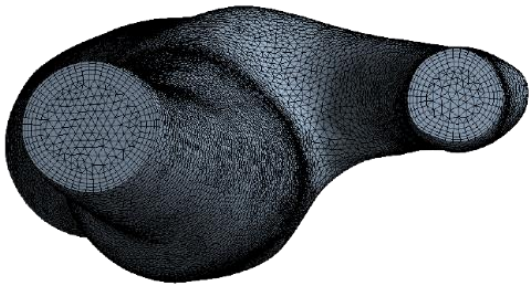

Fig. 8. Boundary layer at the outlet of the carotid artery

Based on the mesh-independence study, the result shows that the lower the body sizing, the higher the number of elements (i.e., from 778187 to 1076057) and it increases the maximum velocity at the ICA outlet from 1.026 ms^{-1} to 1.039 ms^{-1}.

Based on Table 2, the percentage error is 0.19% which is less than 1% for body sizing of 0.24 m on the maximum velocity produced. Thus, 0.24 m body sizing is used for the blood flow simulation in order to reduce the mesh influence while optimizing computational effort and runtime.

Table 2
Mesh-independence study for ICA outlet

Mesh Sizing (m)	No. Elements	Maximum Velocity (ms^{-1})
0.26	778187	1.026
0.25	900051	1.029
0.24	961566	1.039
0.23	1076057	1.039

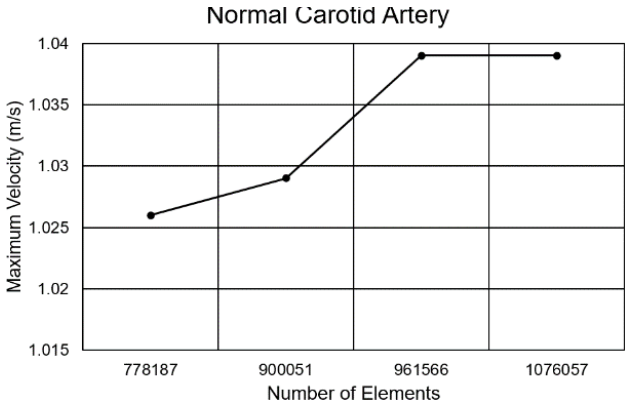

Fig. 9. Mesh independence study for the simulation

For this study, the turbulence model used is SST k-ω with low Reynold's correction. The studies tested several turbulence models in order to justify the most reliable blood flow simulation result. Few turbulence models that were used are standard *k-ε*, SST *k-ω*, and SST *k-ω* with low Reynolds number correction. The study showed that the turbulence model of SST *k-ω* with low Reynolds correction simulated a reasonable range of velocity magnitude for the normal geometry of the carotid artery. For acoustic boundary conditions, the simulation used a broadband noise source model. In terms of model parameters, speed of sound in the blood is 1570 ms^{-1} and the reference acoustic power used is 350 mW [5,18].

3. Results and Discussion

3.1 Blood Flow Simulation

The results begin with validating the blood flow simulation for a normal carotid artery that uses normal viscosity (which is 0.004 $kgms^{-1}$) in order to produce a reliable effect of different degrees of stenosis as well as the acoustic result. The simulation starts with the case of a normal/healthy carotid artery that has no stenosis at all. This is done to validate the result of the current blood flow simulation with those from Lopes *et al.,* [6]. The comparison is made with Lopes *et al.,* [6] as their study used the same geometry as shown in Figure 10.

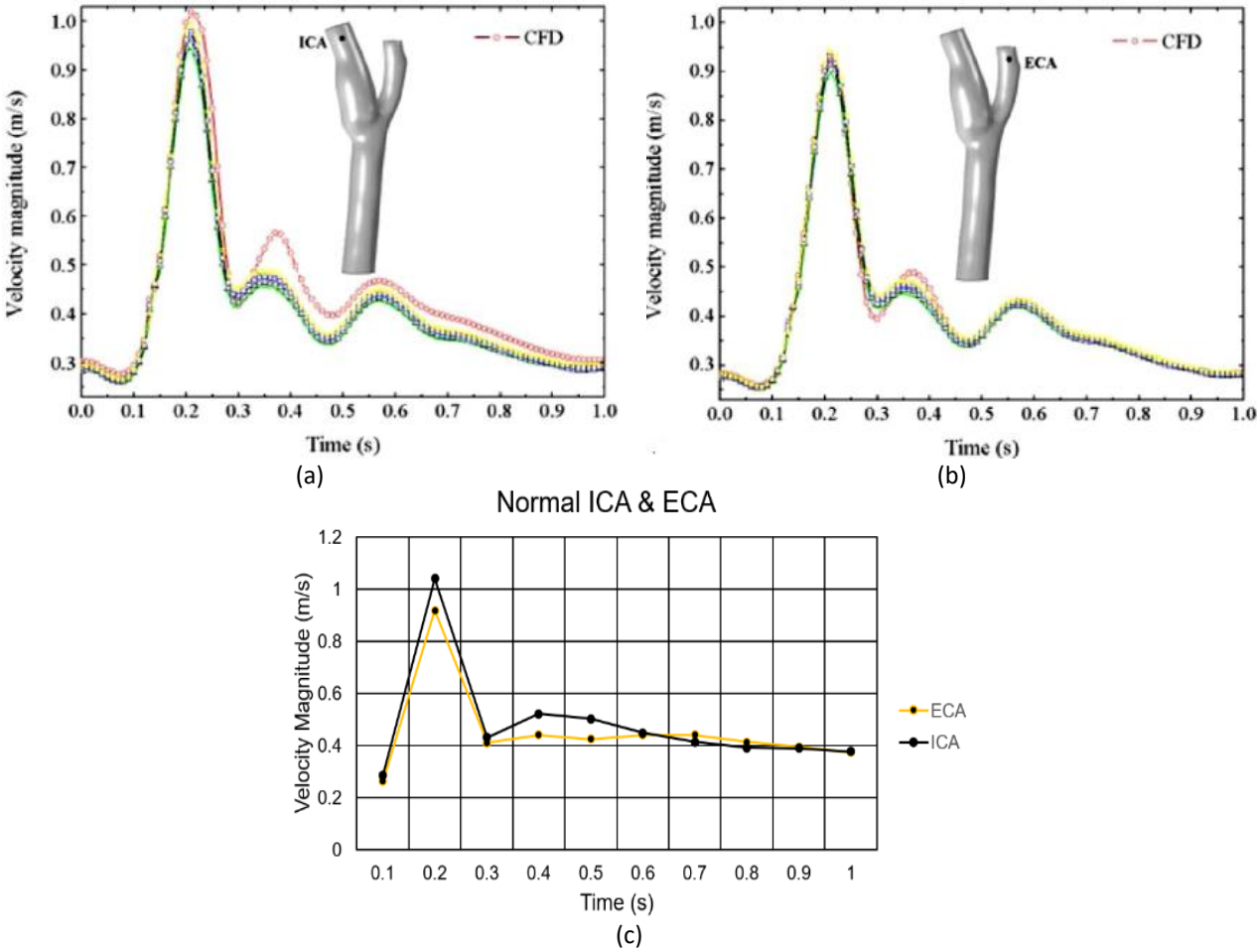

Fig. 10. Comparison of velocity magnitudes at ICA and ECA outlets from Lopes *et al.,* [6] (CFD results represented by red curve in (a) and (b)) with present simulation (c)

Figure 10(a) and Figure 10(b) show the result of velocity magnitude against time on ICA and ECA outlets from Lopes *et al.,* [6]. Figure 10(c) shows the present numerical result of ICA velocity which has a slightly higher peak systolic velocity than ECA at 0.2 s. Based on the result, it can be seen that it is the same as those found by Lopes *et al.,* [6], but slightly different at a certain time after peak systolic (0.2 s) which then gradually decreases to initial velocity. Closer examination indicates that the difference between the present simulation and results in a study by Lopes *et al.,* [6] is approximately 15% (max.) in the ICA, suggesting good agreement on the ICA branch. While in the ECA, the difference in velocity is less than 10% (max.) during the first half of the cardiac cycle and may reach up to 38% (max.) nearing the end of the cardiac cycle, where the velocities are already low. However, during the important systolic peak (when velocities are highest and flow-acoustics may be better heard), the difference is approximately 2% in the ECA branch. The difference may be caused by the different usage of boundary conditions for example the pulsatile inlet velocity and type of turbulence model used. As few significant points are similar with Lopes *et al.,* [6] especially the range of peak velocity for ICA and ECA outlet, the present result is validated. Next, the effect of different degrees of stenosis, as well as the acoustic result, are presented.

3.2 Effect of Different Degrees of Stenosis

Alteration on the normal/healthy geometry of the carotid artery were made corresponding to 30% and 70% degree of stenosis as shown in Figure 11 and Figure 12. Based on the simulation result that has been made, the different degrees of stenosis do affect the velocity of the blood flow as well as the flow acoustics generated. A parabolic (or fully developed) velocity profile is observed at the inlet.

The velocity profile has a maximum value at the center of the segment and gradually decreases as it approaches the wall, in which the velocity is zero as shown in Figure 13. The profile stays thus until it is distorted, which causes the majority of the fluid to flow along the interior walls. Higher velocity can increase the wall shear stress and will potentially damage the endothelial cells on the wall of the blood vessel. As a consequence, the development of stenosis will increase.

$$Re = \frac{\rho V D}{\mu} \tag{2}$$

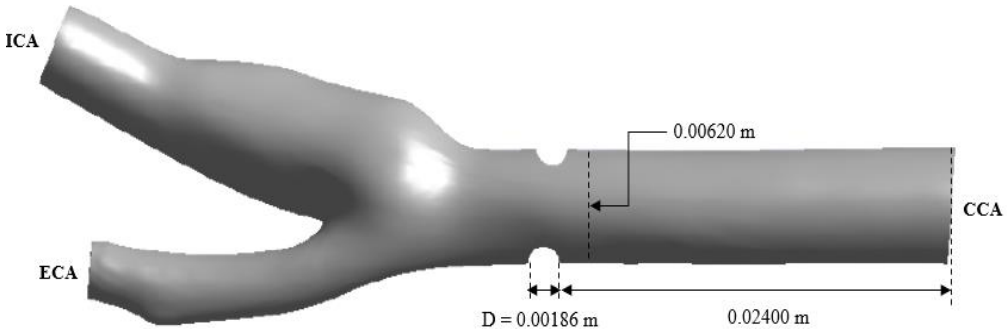

Fig. 11. Dimensions for 30% degree of stenosis

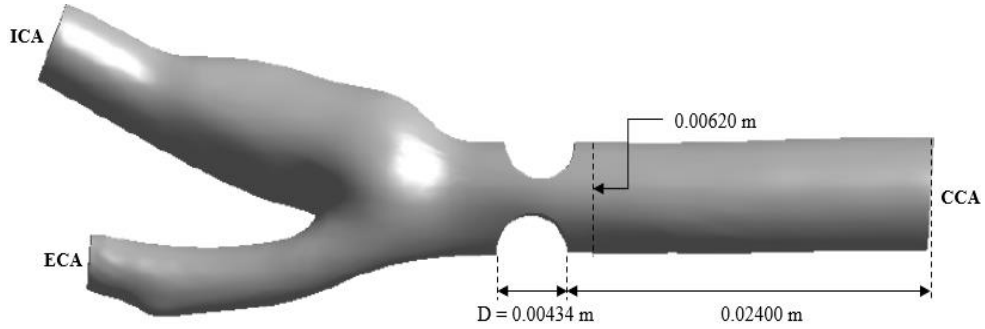

Fig. 12. Dimensions for 70% degree of stenosis

Based on the result obtained, the higher the degree of stenosis from 30% to 70%, the higher the velocity produced. This can satisfy the Reynolds equation where velocity and diameter are inversely proportional, it means that as the diameter from stenosis-to-stenosis decreases, the velocity increases as shown in Eq. (2). It can be seen that at the velocity contour of 0.2 s (which the systolic peaks), the maximum velocity contour (in red) is dominating the majority of velocity contour at the center on both ICA and ECA outlet for all geometry as shown in Figure 15. After the systolic peak, the maximum velocity is not decreasing rapidly, but it continually decreases in a slow progression until it reaches the initial maximum velocity back at time 0.1 s. The maximum velocity changes for ICA at the systolic peak from normal to 70% degree of stenosis for carotid artery is increasing by 8% while opposite trend happened to the maximum velocity changes for ECA at the systolic peak from normal to 70% degree of stenosis for carotid artery (where a reduction of 3% is observed). Thus, it shows that the difference may be caused by the effect of the bifurcating geometry as well as the different location of stenosis. As shown in Figure 13, the maximum velocity occurs at the throat of the stenosis and as the degree of stenosis increases from normal to 70%, the velocity is increasing.

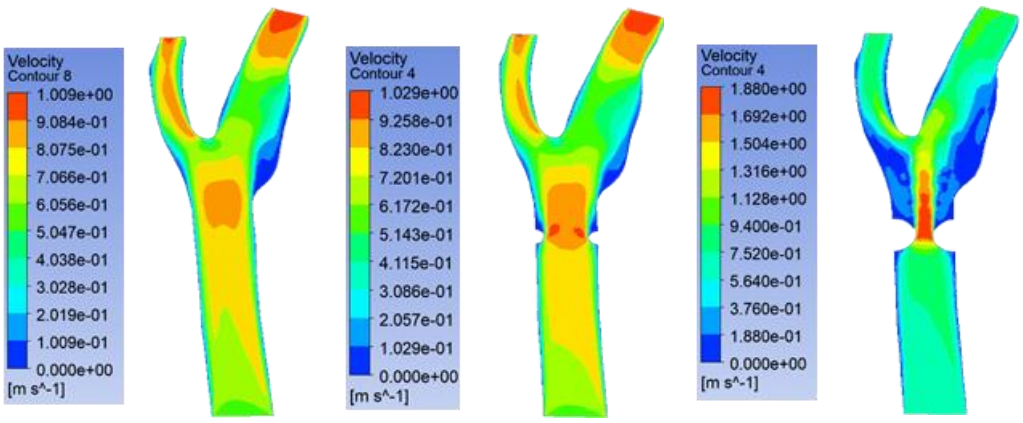

(a) (b) (c)

Fig. 13. Velocity contour for (a) normal stenosis (b) 30% stenosis (c) 70% stenosis of blood flow along the carotid artery at systolic peak (0.2 s)

3.3 Effect of High Blood Viscosity

High viscosity or hyperglycemia is imposed on the blood property by increasing the viscosity from 0.004 $kgms^{-1}$ (normal) to 0.005 $kgms^{-1}$ (hyperviscosity). Based on the simulation result shown in Table 3, the ICA outlet systolic peak velocity at 0.2 s decreases from 1.039 ms^{-1} to 1.029 ms^{-1} as the viscosity increases. However, this does not happen to the velocity for the ECA outlet as shown in Table 4, where the velocity is decreasing. This result can be validated because it matches the result from Bouteloup *et al.,* [4] where higher viscosity does decrease the velocity of the blood flow. In terms of the effect of hyperviscosity in the blood, the maximum velocity changes for ICA at systolic peak for carotid artery is decreasing for normal and 30% degree of stenosis (i.e., 1% and 3%, respectively) but for 70% degree of stenosis, the maximum velocity increases by 7%. On the ECA, a different trend is observed during systolic peak for each degree of stenosis from normal, 30% and 70% for carotid artery, where maximum velocity increases by 9%, 3% and 4%, respectively.

Table 3
Velocity comparison between normal and hyperviscosity for ICA at 0.2 s

Geometry	Velocity magnitude for normal viscosity (m/s)	Velocity magnitude for hyperviscosity (m/s)
Normal	1.039	1.029
30%	1.040	1.010
70%	1.033	1.109

Table 4
Velocity comparison between normal and hyperviscosity for ECA at 0.2 s

Geometry	Velocity magnitude for normal viscosity (m/s)	Velocity magnitude for hyperviscosity (m/s)
Normal	0.918	1.004
30%	0.934	0.965
70%	0.936	0.970

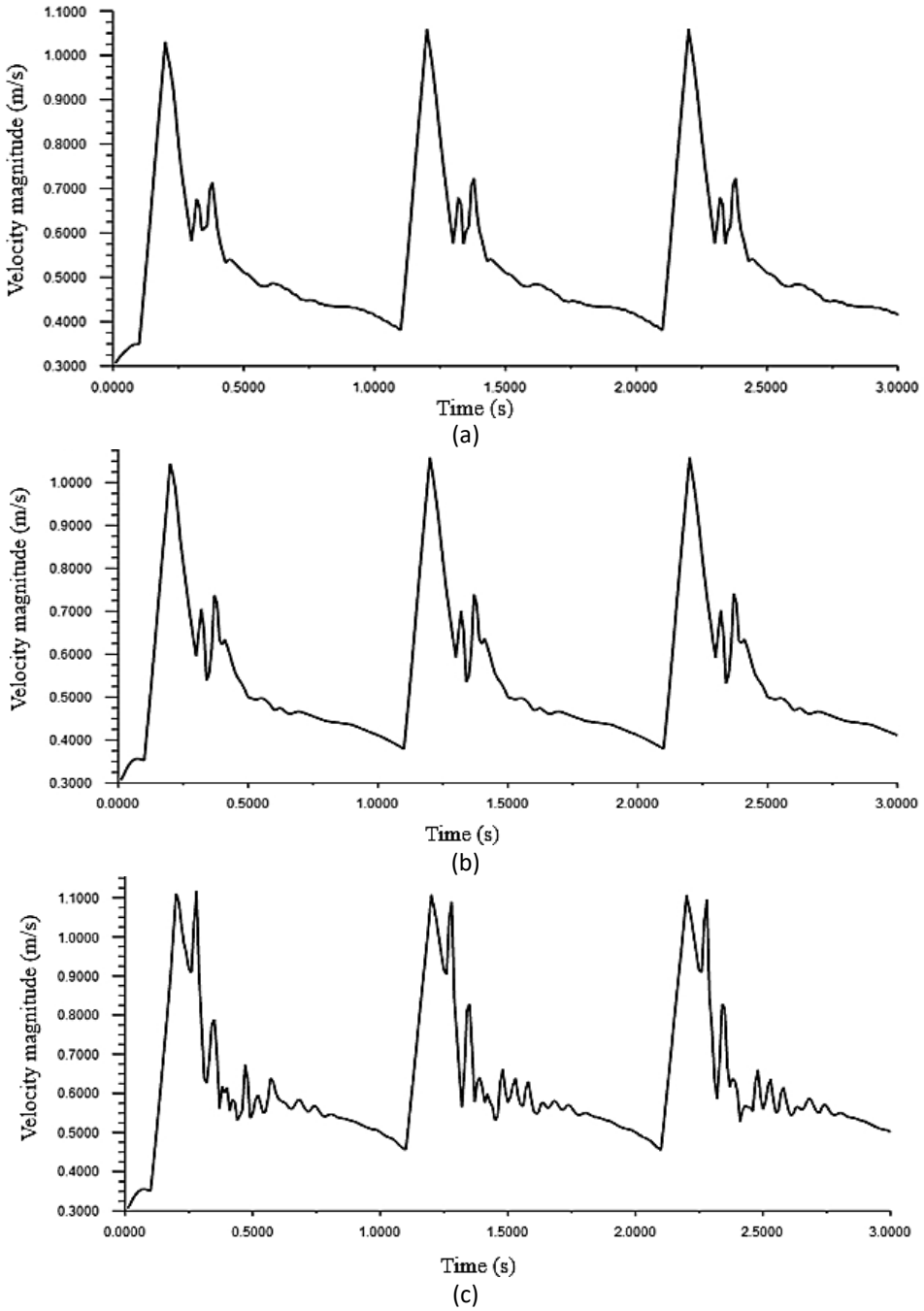

Fig. 14. Velocity magnitude against time at ICA outlet for (a) normal (b) 30% stenosis (c) 70% stenosis geometry

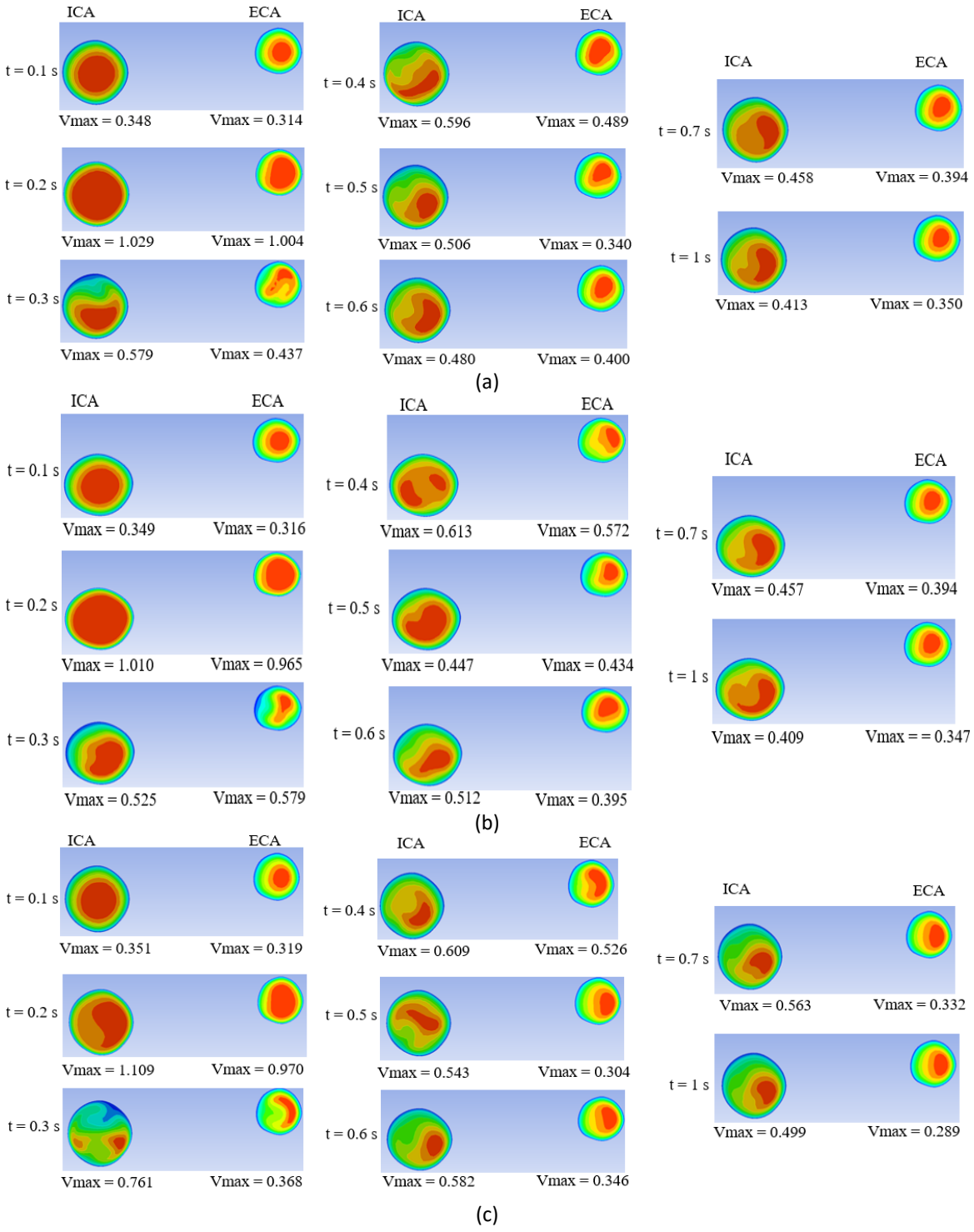

Fig. 15. Velocity contour for ICA and ECA outlet for (a) normal geometry (b) 30% degree of stenosis (c) 70% degree of stenosis

3.4 Acoustics Characteristics Generated

It is proven that clogging in the blood vessel can increase the Reynolds number until it reaches turbulence and even higher. As the blood flow is turbulent, more fluctuation will occur, and aggressive acoustic will produce. Based on Table 5, the higher the degree of pre-bifurcation stenosis from normal, 30% and 70%, the higher the value of the acoustic power produced. However, when the level of viscosity is increased, it is noticeable that the acoustic power increased by 5% and 20%

for geometry that has 30% and 70% degree of stenosis, respectively. However, this is not the case for normal geometry, where it just slightly increased by 0.14% as the viscosity increased. Figure 16(a) shows the relationship for acoustic power against degree of stenosis, with correlation R^2 = 0.9823. The closer the R^2 value to 1, the better the correlation.

Based on Table 6, the higher the degree of pre-bifurcation stenosis for normal, 30% and 70%, the higher the value of the surface acoustic strength generated. Similarly, when the level of viscosity is increased, it can be seen that acoustic surface power increases in all geometry. Figure 16(b) shows the correlation R^2 for acoustic surface power against degree of stenosis i.e., R^2 = 0.819, which again is almost 1. Thus, the correlation is close to be accepted.

Table 5
Comparison of acoustic power for normal viscosity and hyperviscosity

Geometry	Maximum acoustic power for normal viscosity (W/m^3)	Maximum acoustic power for hyperviscosity (W/m^3)
Normal	6.73e-25	6.74e-25
30%	3.66e-37	5.53e-23
70%	3.65e-37	1.01e-22

Table 6
Comparison of surface acoustic power for normal viscosity and hyperviscosity

Geometry	Maximum surface acoustic power for normal viscosity (W/m^2)	Maximum surface acoustic power for hyperviscosity (W/m^2)
Normal	4.848e-11	1.010e-10
30%	4.848e-11	1.014e-10
70%	4.848e-11	2.070e-10

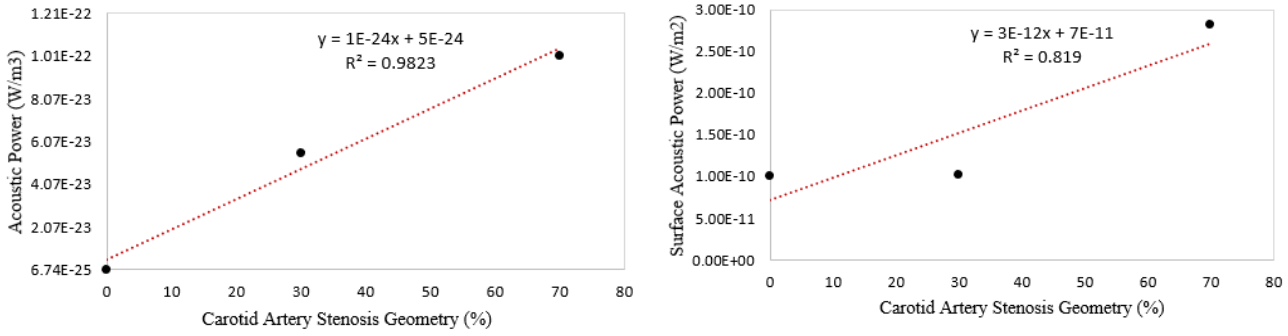

Fig. 16. Correlation between acoustics and varying degree of carotid artery stenosis (a) acoustic power (b) surface acoustic power

Figure 17 and Figure 18 shows contour of the acoustic power along a mid-plane and surface of the carotid artery respectively, under varying degrees of stenosis. The plots show that acoustic power increases with narrowing in the carotid artery. In particular, high level of acoustics are observed near the stenosed regions.

The proposed relationship indicates a positive correlation between degree of stenosis with acoustic power generated, as indicated by the positive R^2 value that is close to 1.0. This may be exploited to help estimate or measure the severity of stenosis in the carotid artery based on the flow acoustics generated. Indeed, further work is required to further refine or develop this approach where potentially, the acoustic signals generated may be measured and characterised, and used to correlate or measure the degree of stenosis in the carotid artery.

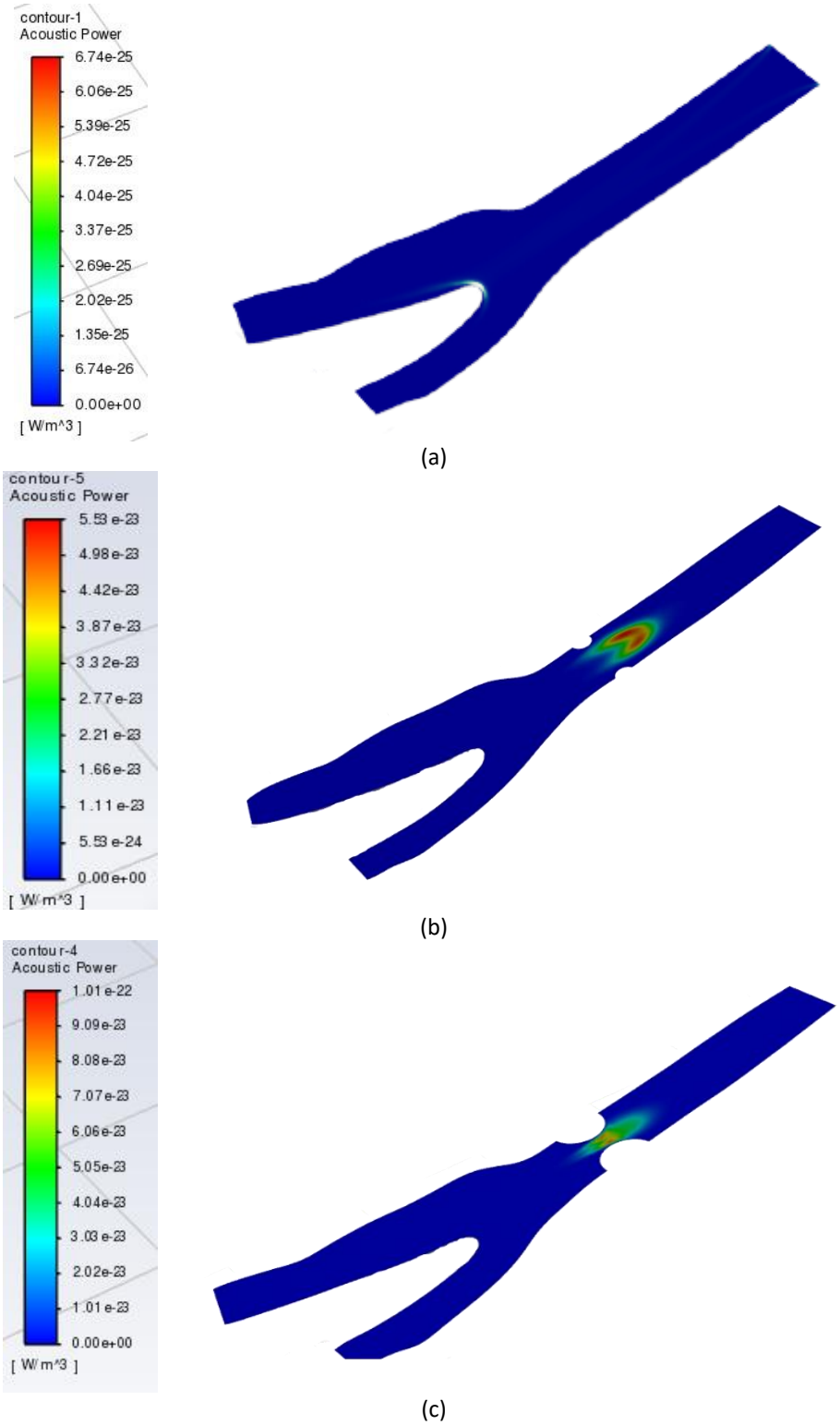

Fig. 17. Acoustic power contour of carotid artery for (a) normal geometry (b) 30% degree of stenosis (c) 70% degree of stenosis

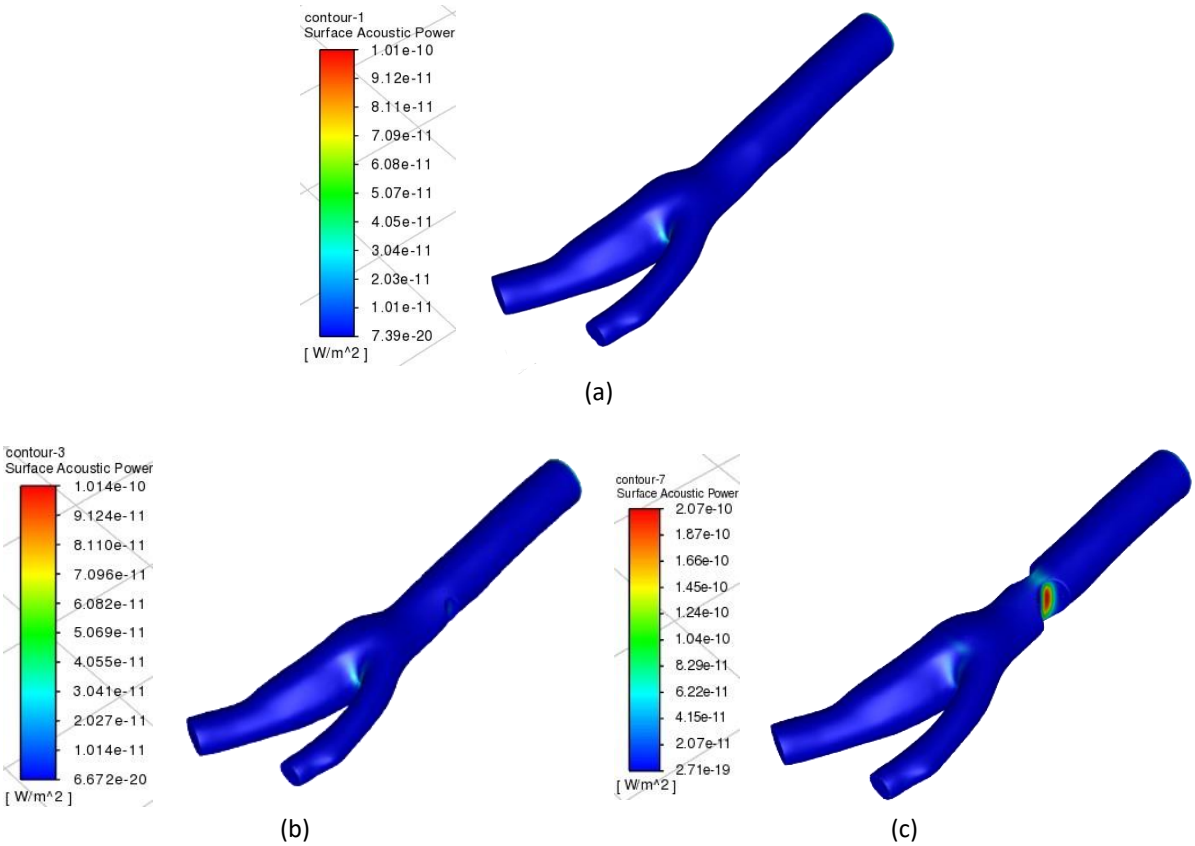

Fig. 18. Surface acoustic power for (a) normal geometry (b) 30% degree of stenosis (c) 70% degree of stenosis

4. Conclusions

A computational investigation was undertaken to study the effect of different degrees of pre-bifurcation stenosis and blood viscosity, specifically towards the blood flow characteristics and the acoustic generated. Based on the result obtained from the CFD simulations, it may be concluded that different degrees of stenosis, as well as hyperglycemia, do affect the blood flow characteristics and acoustics generated in the carotid artery. In terms of the hyperviscosity used, although it did change the velocity of the blood flow, the percentage difference was less than 10%. For the acoustics, the result showed that as the degree of stenosis increases, the acoustic power and surface acoustic power increases, especially with increase in viscosity. A mathematical relationship is proposed, showing a positive correlation between the acoustic power and degree of stenosis in the carotid artery. This may be potentially be further developed and refined to help detect and estimate the degree of narrowing in the carotid artery by a non-invasive acoustical means, which may perhaps be cheaper and more practical than the current diagnosis practice. Indeed, the present work is in its initial stage and further study is necessary. Future works including simulating different shapes of stenosis, post-bifurcation stenosis and wider range of blood viscosity that may be found in the population, are required to further develop and refine the present study.

Acknowledgement
The authors would like to thank all those involved in making this study a success, and acknowledge support from grant FRGS/1/2018/TK03/UKM/02/5 funded by the Ministry of Higher Education, Malaysia.

References

[1] Lopez, Alan D., Colin D. Mathers, Majid Ezzati, Dean T. Jamison, and Christopher J. L. Murray. "Global and regional burden of disease and risk factors, 2001: systematic analysis of population health data." *The Lancet* 367, no. 9524 (2006): 1747-1757. https://doi.org/10.1016/S0140-6736(06)68770-9

[2] Blaser, Till, Katrin Hofmann, Thomas Buerger, Olaf Effenberger, Claus-Werner Wallesch, and Michael Goertler. "Risk of stroke, transient ischemic attack, and vessel occlusion before endarterectomy in patients with symptomatic severe carotid stenosis." *Stroke* 33, no. 4 (2002): 1057-1062. https://doi.org/10.1161/01.STR.0000013671.70986.39

[3] Khalili, Fardin, Peshala PT Gamage, Ibrahim A. Meguid, and Hansen A. Mansy. "A coupled CFD-FEA study of the sound generated in a stenosed artery and transmitted through tissue layers." In *SoutheastCon 2018*, pp. 1-6. IEEE, 2018. https://doi.org/10.1109/SECON.2018.8478873

[4] Bouteloup, Hugo, Johann Guimaraes de Oliveira Marinho, and Daniel M. Espino. "Computational analysis to predict the effect of pre-bifurcation stenosis on the hemodynamics of the internal and external carotid arteries." *Journal of Mechanical Engineering and Sciences* 14, no. 3 (2020): 7029-7039. https://doi.org/10.15282/jmes.14.3.2020.05.0550

[5] Seo, Jung Hee, and Rajat Mittal. "A coupled flow-acoustic computational study of bruits from a modeled stenosed artery." *Medical & Biological Engineering & Computing* 50, no. 10 (2012): 1025-1035. https://doi.org/10.1007/s11517-012-0917-5

[6] Lopes, D., Hélder Puga, J. Carlos Teixeira, and S. F. Teixeira. "Influence of arterial mechanical properties on carotid blood flow: Comparison of CFD and FSI studies." *International Journal of Mechanical Sciences* 160 (2019): 209-218. https://doi.org/10.1016/j.ijmecsci.2019.06.029

[7] Chen, Zimo, Haiqiang Qin, Jia Liu, Bokai Wu, Zaiheng Cheng, Yong Jiang, Liping Liu et al. "Characteristics of wall shear stress and pressure of intracranial atherosclerosis analyzed by a computational fluid dynamics model: a pilot study." *Frontiers in Neurology* 10 (2020): 1372. https://doi.org/10.3389/fneur.2019.01372

[8] Zakaria, Mohamad Shukri, Farzad Ismail, Masaaki Tamagawa, Ahmad Fazli Abdul Azi, Surjatin Wiriadidjaya, Adi Azrif Basri, and Kamarul Arifin Ahmad. "Computational fluid dynamics study of blood flow in aorta using OpenFOAM." *Journal of Advanced Research in Fluid Mechanics and Thermal Sciences* 43, no. 1 (2018): 81-89.

[9] Khader, Shah Mohammed Abdul, Adi Azriff, Cherian Johny, Raghuvir Pai, Mohammad Zuber, Kamarul Arifin Ahmad, and Zanuldin Ahmad. "Haemodynamics behaviour in normal and stenosed renal artery using computational fluid dynamics." *Journal of Advanced Research in Fluid Mechanics and Thermal Sciences* 51, no. 1 (2018): 80-90.

[10] Dabagh, Mahsa, Paritosh Vasava, and Payman Jalali. "Effects of severity and location of stenosis on the hemodynamics in human aorta and its branches." *Medical & Biological Engineering & Computing* 53, no. 5 (2015): 463-476. https://doi.org/10.1007/s11517-015-1253-3

[11] Lopes, D., H. Puga, J. Teixeira, and R. Lima. "Blood flow simulations in patient-specific geometries of the carotid artery: A systematic review." *Journal of Biomechanics* 111 (2020): 110019. https://doi.org/10.1016/j.jbiomech.2020.110019

[12] Al-Azawy, Mohammed Ghalib, Saleem Khalefa Kadhim, and Azzam Sabah Hameed. "Newtonian and Non-Newtonian Blood Rheology Inside a Model of Stenosis." *CFD Letters* 12, no. 11 (2020): 27-36. https://doi.org/10.37934/cfdl.12.11.2736

[13] Mahrous, Samar A., Nor Azwadi Che Sidik, and Khalid M. Saqr. "Newtonian and non-Newtonian CFD models of intracranial aneurysm: a review." *CFD Letters* 12, no. 1 (2020): 62-86.

[14] Sarifuddin. "CFD modelling of Casson fluid flow and mass transport through atherosclerotic vessels." *Differential Equations and Dynamical Systems* (2020). https://doi.org/10.1007/s12591-020-00522-y

[15] Yusof, Nur Syamila, Siti Khuzaimah Soid, Mohd Rijal Illias, Ahmad Sukri Abd Aziz, and Nor Ain Azeany Mohd Nasir. "Radiative Boundary Layer Flow of Casson Fluid Over an Exponentially Permeable Slippery Riga Plate with Viscous Dissipation." *Journal of Advanced Research in Applied Sciences and Engineering Technology* 21, no. 1 (2020): 41-51. https://doi.org/10.37934/araset.21.1.4151

[16] Ku, D. N., D. P. Giddens, D. J. Phillips, and D. E. Strandness Jr. "Hemodynamics of the normal human carotid bifurcation: in vitro and in vivo studies." *Ultrasound in Medicine & Biology* 11, no. 1 (1985): 13-26. https://doi.org/10.1016/0301-5629(85)90003-1

[17] Lee, Seung E., Sang-Wook Lee, Paul F. Fischer, Hisham S. Bassiouny, and Francis Loth. "Direct numerical simulation of transitional flow in a stenosed carotid bifurcation." *Journal of Biomechanics* 41, no. 11 (2008): 2551-2561. https://doi.org/10.1016/j.jbiomech.2008.03.038

[18] Zauhar, G., H. C. Starritt, and F. A. Duck. "Studies of acoustic streaming in biological fluids with an ultrasound Doppler technique." *The British Journal of Radiology* 71, no. 843 (1998): 297-302. https://doi.org/10.1259/bjr.71.843.9616239